ORIGINAL PAPER

Post-peak behaviour of rocks under cyclic loading using a double-criteria damage-controlled test method

Roohollah Shirani Faradonbeh[1] • **Abbas Taheri**[1] • **Murat Karakus**[1]

Abstract

Cyclic loading–induced hazards are severe instability problems concerning surface and underground geotechnical projects. Therefore, it is crucial to understand the rock failure mechanism under cyclic loading. An innovative double-criteria damage-controlled testing method was proposed in this study to capture the complete stress–strain response of porous limestone, especially the post-peak behaviour, under systematic cyclic loading. The proposed test method was successful in applying the pre-peak cyclic loading and then in controlling the self-sustaining failure of rock during the post-peak cyclic loading. The results showed that the strength of the rock specimens slightly increased with an increase in the fatigue life in the pre-peak region due to cyclic loading–induced hardening. Additionally, a combination of class I and class II behaviours was observed in the post-peak region during the cyclic loading tests; the class II behaviour was more dominant by the increase in fatigue life in the pre-peak region. Damage evolution was assessed based on several parameters, such as the elastic modulus, energy dissipation ratio, damage variable and crack damage threshold stress, both in the pre-peak and post-peak regions. It was found that when the cyclic loading stress is not close to the peak strength, due to a coupled mechanism of dilatant microcracking and grain crushing and pore filling, quasi-elastic behaviour dominates the cyclic loading history, causing more elastic strain energy to accumulate in the specimens.

Keywords Cyclic loading · Pre-peak and post-peak behaviour · Damage · Crack damage threshold stress · Strength hardening

Introduction

Surface and underground structures are usually exposed to environmental and human-induced cyclic loadings such as earthquakes, wind, volcanism, drilling and blasting, mechanical excavation and mining seismicity, which threaten their long-term stability (Taheri et al. 2016; Munoz et al. 2016a). Therefore, it is necessary to evaluate the time-dependent behaviour of rocks under cyclic loading. In rock engineering, understanding the fatigue response of rocks is of particular interest since rock stability conditions vary significantly under cyclic loading. A great majority of rock fatigue studies have reported on the reduction in rock strength due to cyclic loading (Bagde and Petroš 2005). However, there are very few studies that have illustrated strength hardening when the cyclic stress level is low enough to prevent failure during cyclic loading (Burdine 1963; Singh 1989; Ma et al. 2013; Taheri et al. 2017). Unlike the static and quasi-static loadings, in which the applied load/deformation increases/decreases continuously, cyclic loading is described by a time-dependent displacement/load signal with a repetitive pattern. The loading rate in cyclic experiments is relatively high and propagates waves, and their superposition causes a stress distribution different from that induced by quasi-static loading (Cho et al. 2003). In recent decades, many studies have investigated the mechanical behaviour of rocks under different cyclic loading histories and loading conditions. Most of these studies have reported the results of tests performed under uniaxial compression (Attewell and Sandford 1974; Eberhardt et al. 1999), which can replicate the stress state in mining pillars and around galleries. Other studies have focused on triaxial

✉ Roohollah Shirani Faradonbeh
roohollah.shiranifaradonbeh@adelaide.edu.au

Abbas Taheri
abbas.taheri@adelaide.edu.au

Murat Karakus
murat.karakus@adelaide.edu.au

1   School of Civil, Environmental and Mining Engineering, The University of Adelaide, Adelaide, SA 5005, Australia

compression conditions with different confining pressures (Munoz et al. 2016a; Zhou et al. 2019) and indirect tensile tests (Ghamgosar and Erarslan 2016), which are useful to calibrate the advanced constitutive laws and to estimate the tensile strength of a material, respectively. In addition, few cyclic studies of flexural tests (three-point and four-point) (Cardani and Meda 2004) and freeze-thaw tests (Zhang et al. 2019a) can be found in the literature. In prior studies, the fatigue properties of rocks were found to be dependent on the loading stress level, amplitude, frequency, waveform and loading and unloading rate.

Rock behaviour in the post-peak region under uniaxial compression is characterised by either class I or class II behaviour (Fig. 1). The former is defined by a negative post-peak modulus describing a stable fracture propagation and the need to do more work on the specimen to degrade its load-bearing capacity, while the latter represents a positive post-peak modulus (i.e. snap-back behaviour) describing a self-sustaining (brittle) failure (Wawersik and Fairhurst 1970; Munoz et al. 2016b). The proper measurement of the post-peak behaviour of rocks can be a useful tool for quantifying the post-peak fracture energy and rock brittleness that can be employed to optimise the designation of surface and underground structures and to mitigate possible hazards (Akinbinu 2016). For instance, to evaluate the proneness and intensity of the rock burst phenomenon near underground excavation in deep underground conditions, post-peak analysis of the rocks in terms of strain energy evolution is required. In other words, the rock burst hazard in deep underground openings is associated with not only internal strain energy accumulation but also seismic disturbances induced by external sources (Xuefeng et al. 2010). Therefore, the post-peak response of rocks subjected to cyclic loading can unveil the
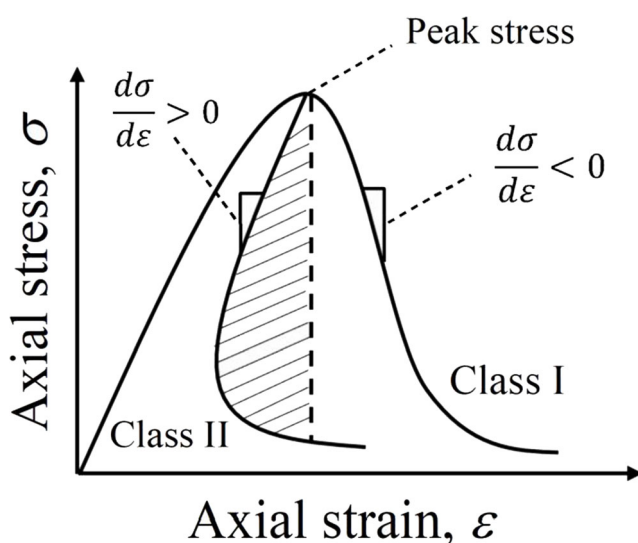
mechanism of geotechnical hazards such as rock burst and provide practical tools for their assessment. As shown in Fig. 2, the cyclic loading of rock can be undertaken following two main loading methods:

1. Systematic cyclic loading: These tests have a constant loading amplitude, Amp. (σ_a), and can be conducted as single-level (Fig. 3a) or multi-level (Fig. 3b) tests under load-controlled or displacement-controlled (i.e. axial and lateral displacement–controlled) loading conditions. In both load-controlled and displacement-controlled conditions, the post-peak behaviour cannot be obtained, as the axial load level is the only criterion to define the amount of the load that a specimen should be subjected to during cyclic loading, until failure or even after failure. As a result, the specimen fails during cyclic loading in an uncontrolled manner, and the post-peak response cannot be obtained. Figure 4 a–d demonstrate the single-level and multi-level systematic cyclic tests conducted by different researchers under load-controlled and displacement-controlled conditions. As shown in these figures, in all the tests, failure occurred in an uncontrolled manner, and post-peak behaviour was not obtained. Prior systematic cyclic loading studies found that failure occurs at a stress level lower than the determined monotonic strength owing to the strength weakening process. As such, the accumulation of irreversible deformation (plastic strains) is not constant during the experiment, while the hysteresis loops follow a loose-dense-loose law (Xiao et al. 2009).

2. Damage-controlled cyclic loading: These tests involving incremental loading amplitude can be conducted in a load-based mode (Fig. 3c) or displacement-based mode (Fig. 3d). The former can be conducted either in load-controlled or displacement-controlled loading conditions (i.e. axial and lateral displacement–controlled). However, the post-peak response cannot be obtained, as the specimen might experience an uncontrolled failure when it is forced to reach a pre-defined stress level. Figure 4 e and f show representative results. A displacement-based test can be undertaken in either axial or lateral displacement–controlled conditions. In this type of damage-controlled test, axial stress is reversed when a certain amount of axial or lateral displacement is achieved in a loading cycle. Munoz et al. (2016b) showed that under uniaxial loading conditions, soft, medium-strong and strong rocks demonstrate either class II or a combination of class I and class II post-peak behaviours. As a result, the post-peak response cannot be adequately measured when the test is controlled by axial displacement (Fig. 4g). However, by using lateral strain to control the amount of damage in a damage-controlled test, the post-peak behaviour of a brittle rock can be achieved successfully (Fig. 4h). From prior damage-controlled cyclic
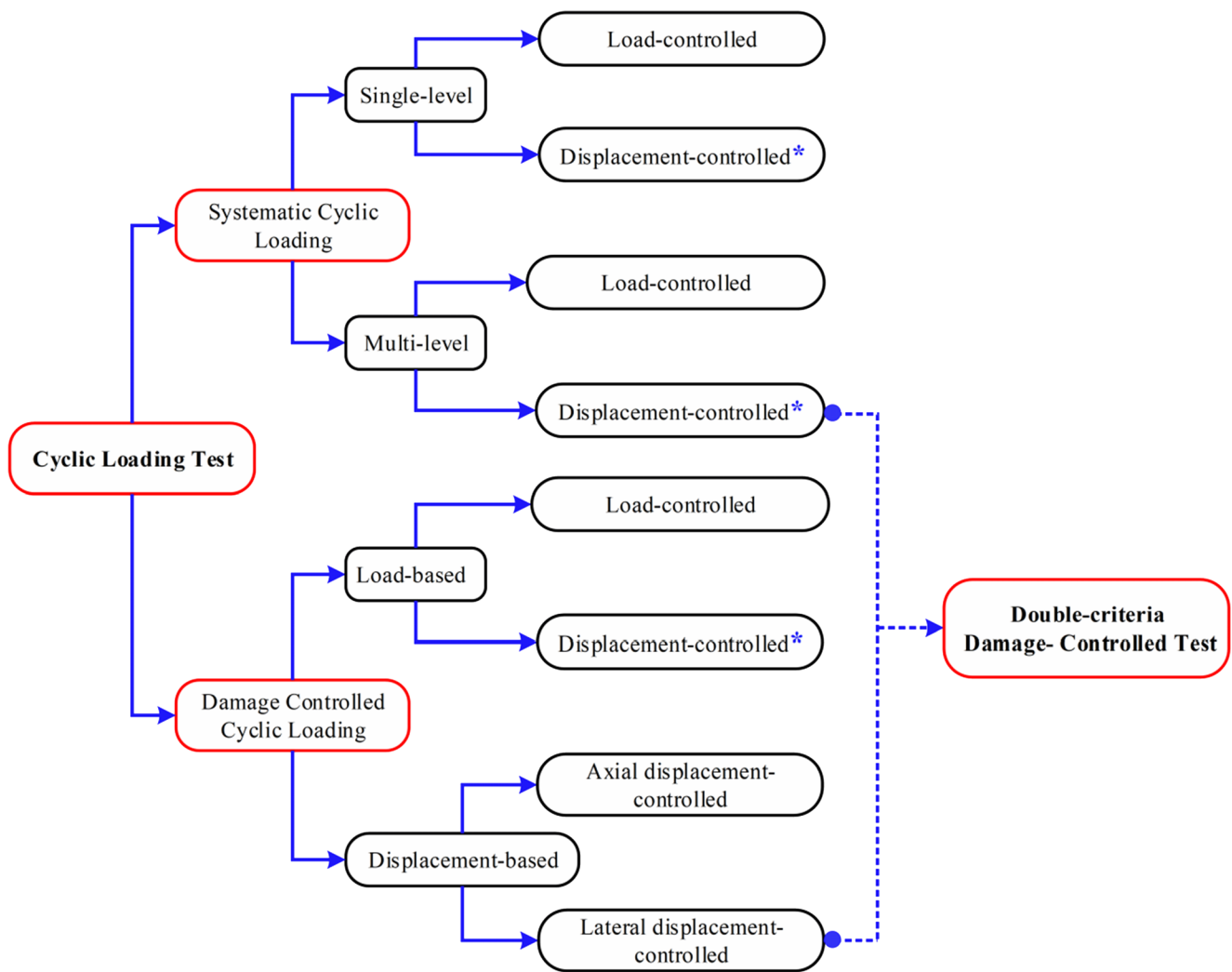

Fig. 1 Classification of post-peak behaviour of rock in uniaxial compression (modified from Hudson et al. 1971)

Fig. 2 Classification of cyclic loading tests. *Can be conducted in either axial or lateral displacement–controlled mode

loading studies, it is reported that failure occurs at a stress level close to or lower than the determined monotonic strength. Moreover, the rate of strain accumulation under this type of loading is lower than that during systematic cyclic tests (Cerfontaine and Collin 2018).

It should be noted that previous studies have mostly focused on the influence of cyclic loadings on the mechanical rock properties and damage evolution in the pre-peak region. There are, however, a few studies investigating failure behaviour and deformation localisation during post-peak cyclic loading (e.g. Munoz and Taheri 2017a, 2019). Given the above, to the best of our knowledge, no study has investigated the post-peak response of rocks subjected to pre-peak systematic cyclic loading. This is because failure cannot be controlled when a constant axial load is achieved in every cycle in a systematic cyclic loading. In addition, in a damage-

controlled test in which the lateral displacement is used to control the damage, an axial load is reversed when a certain amount of lateral strain occurs. Therefore, systematic cyclic loading cannot be applied in such a way that the load is always reversed at a constant stress level in the pre-peak region. However, rock material in engineering applications (e.g. mining pillars in deep underground conditions) may be subjected to systematic pre-peak cyclic loading and then post-failure cyclic loading. Thus, it is significant to investigate the behaviour of rock subjected to this loading condition. In this study, for the first time, a new cyclic test method considering two cyclic loading control criteria is proposed to capture the complete response of rocks, especially the post-peak behaviour, under cyclic loading. The proposed test method is a combination of multi-level systematic cyclic loading and lateral displacement–based damage-controlled cyclic loading to control both the damage and the rate of cyclic loading (see Fig. 2). A critical analysis is carried out to investigate damage
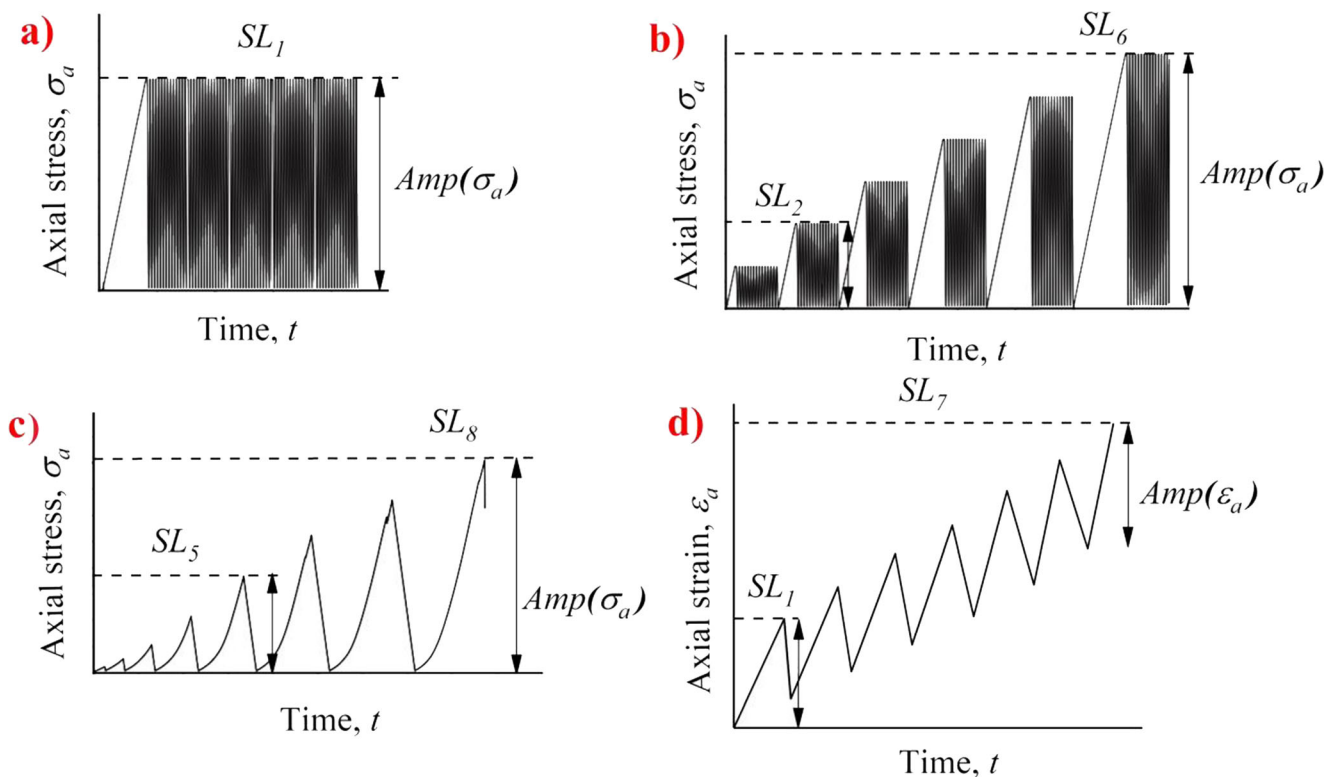
Fig. 3 Different cyclic loading paths. **a** Single-level systematic cyclic loading. **b** Multi-level systematic cyclic loading. **c** Load-based damage-controlled cyclic loading (modified from Li et al. 2019). **d** Displacement-based damage-controlled cyclic loading, Amp. (σ_a) refers to loading amplitude, Amp. (ε_a) refers to axial strain amplitude, and SL refers to the stress level

evolution in both the pre-peak and post-peak regions, and the influences of pre-peak cyclic loading on the peak strength, crack damage threshold stress and rock stiffness are evaluated in more detail.

Experimental methodology

Tuffeau limestone specimens

Tuffeau limestone is used in this study to undertake double-criteria damage-controlled cyclic loading tests (Fig. 5a). The name of this rock comes from the Latin word tofus, meaning spongy rock. This yellowish-white sedimentary rock is a local limestone of the Loire Valley in France and was deposited in the middle Turonian of the Upper Cretaceous, approximately 90 million years ago. This rock type is usually extracted from surface and underground quarries and is used mostly in the building industry (Beck and Al-Mukhtar 2014). X-ray diffraction (XRD) (Fig. 5b) and scanning electronic microscopy (SEM) analyses (Fig. 5c) were carried out on collected limestone specimens to identify their mineralogical components and microstructural characteristics. Two main crystalline phases, calcite ($CaCO_3$) ($\cong 50\%$) and silica (SiO_2) ($\cong 30\%$), which have the two forms of quartz and opal cristobalite-tridymite (opal-CT), were identified. Other phases, such as

mica and clayey minerals (e.g. muscovite, biotite, smectite and glauconite) ($\cong 20\%$), are disseminated in this limestone. Tuffeau limestone has an average density of 1.43 g/cm^3 and is a lightweight and fine-grained limestone with a complex porous network (total porosity of $45 \pm 5\%$). The arrangement of grains with different sizes contributes to the creation of micropores and macropores within the rock texture (Al-Mukhtar and Beck 2006). The rock specimen in Fig. 5c has a heterogeneous porous structure, and the microcracks, microcavities and quartz are the main components controlling the macrofailure of the specimen under loading conditions. The cylindrical rock specimens with diameters and lengths of 42 mm and 100 mm, respectively (i.e. an aspect ratio of 2.4), were cored from a single rock block and prepared to be

Fig. 4 Stress–strain relation during cyclic loading in different studies. **a** ▶ Single-level systematic cyclic loading load-controlled test (Ma et al. 2013). **b** Single-level systematic cyclic loading axial displacement–controlled test (Taheri et al. 2016). **c** Multi-level systematic cyclic loading load-controlled test (Li et al. 2019). **d** Multi-level systematic cyclic loading axial displacement–controlled test (Liu et al. 2014). **e** Load-based damage-controlled cyclic loading load-controlled test (Guo et al. 2018). **f** Load-based damage-controlled cyclic loading axial displacement–controlled test (Heap et al. 2010). **g** Displacement-based damage-controlled cyclic loading axial displacement–controlled test (Wang et al. 2019). **h** Displacement-based damage-controlled cyclic loading lateral displacement–controlled test (Munoz and Taheri 2019)
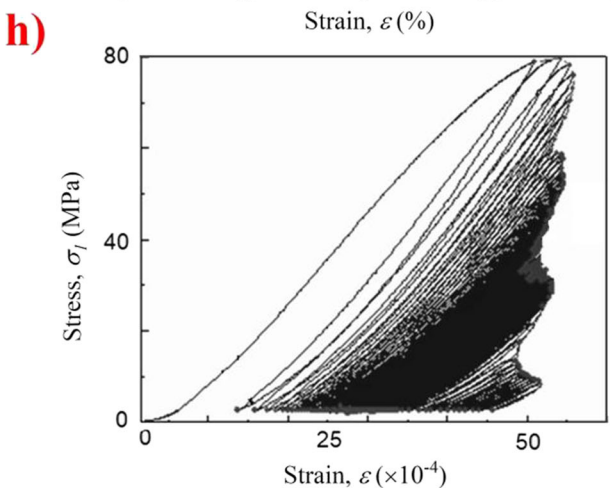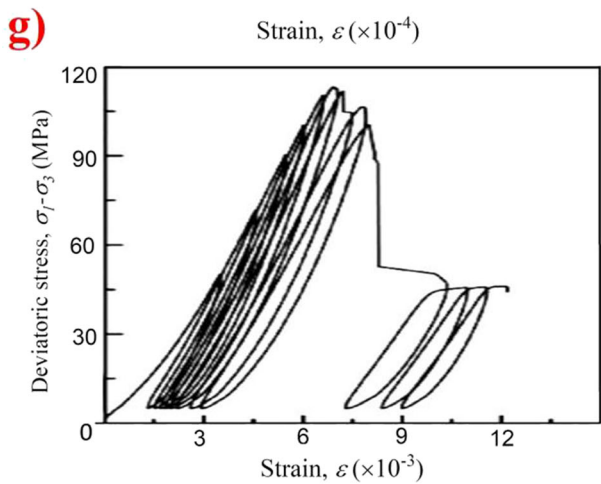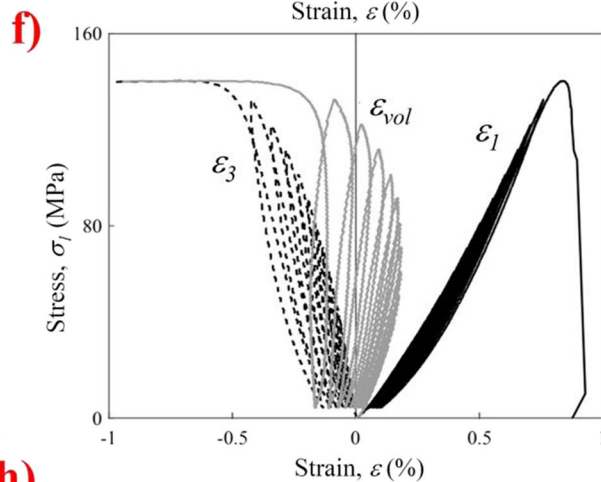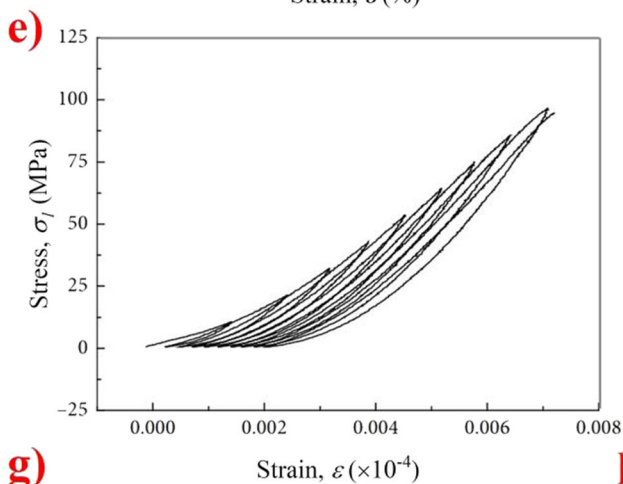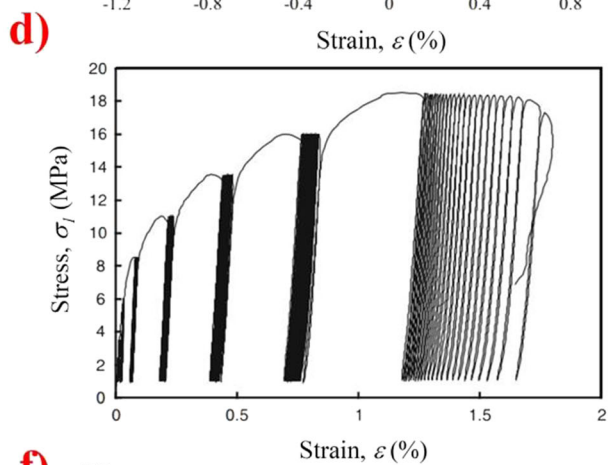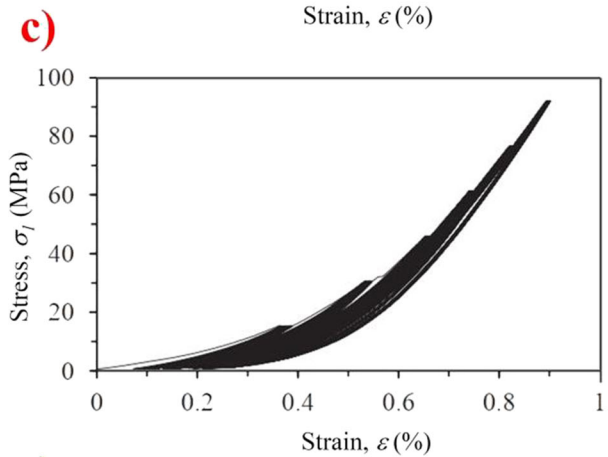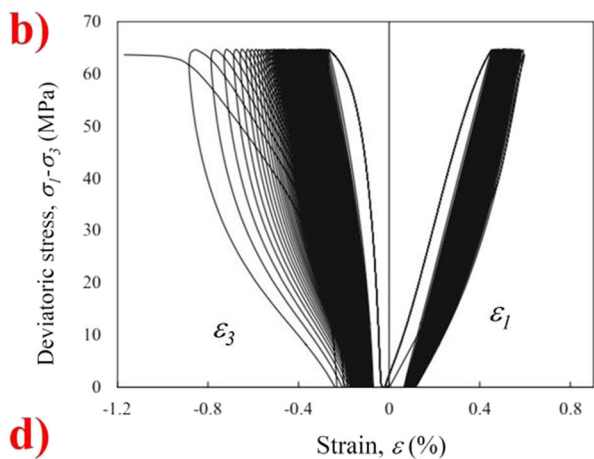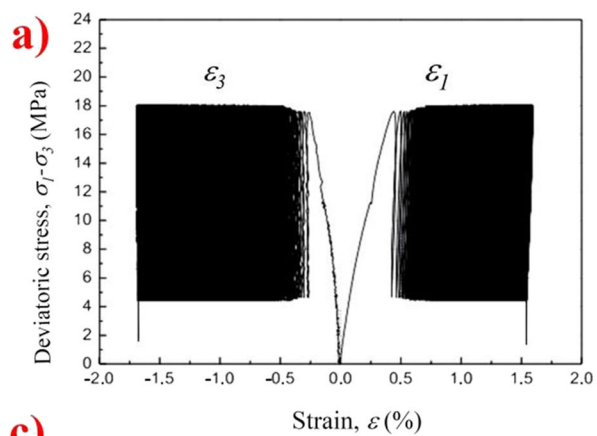
smooth and straight according to the ISRM standards (Fairhurst and Hudson 1999) to minimise the end friction effects and to ensure a uniform stress state within the specimen during loading. Additionally, the diameter of the specimens is more than 20 times larger than the grain size, satisfying the ISRM recommendations (Fairhurst and Hudson 1999).

Test set-up and uniaxial compression tests

In this study, a closed-loop servo-controlled MTS hydraulic compressive machine (Fig. 6a) with a maximum loading capacity of 300 kN was employed to conduct compressive monotonic and cyclic tests. This fully digital servo-controlled system is capable of operating under load- or displacement-control feedback signals using a built-in computer system. In this study, the lateral strain (ε_l) feedback signal measured by a chain extensometer circumferentially

mounted at the mid-length of the specimen was used as the control variable for monotonic and cyclic tests to capture the rock behaviour before and after peak stress. The axial load (acquired by a load cell), axial strain (acquired by a pair of LVDTs) and lateral strain (acquired by a chain extensometer) were recorded simultaneously during the tests by a data acquisition system at a rate of 10 data points per second (see Fig. 6a). Five uniaxial monotonic tests were conducted under the lateral strain rate of 0.02×10^{-4}/s to satisfy the static to quasi-static loading conditions (Munoz and Taheri 2017b). These monotonic tests provide a reference for defining the stress levels of cyclic uniaxial compression tests. The time history of the loading (σ_a), axial strain (ε_a) and lateral strain (ε_l) for a typical monotonic loading test is shown in Fig. 6b. As seen in this figure, in the pre-peak and the post-peak regions, the lateral strain (ε_l) increases monotonically with time, maintaining a constant lateral strain rate throughout the test, and the
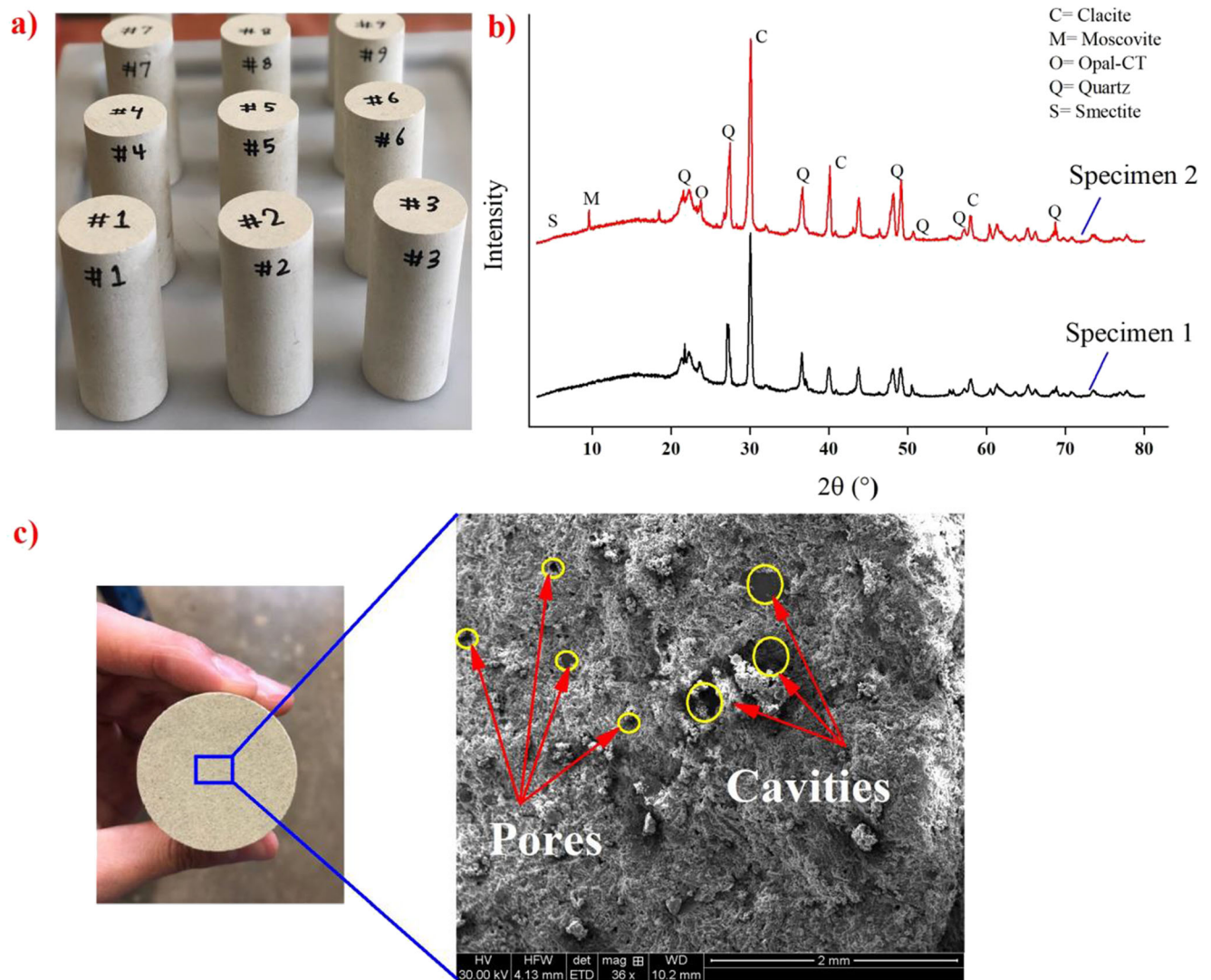

Fig. 5 a Tuffeau limestone specimens. b XRD analysis conducted for two specimens. c SEM photograph showing the diversity of porosities in a tuffeau limestone specimen

Fig. 6 **a** Testing set-up for the uniaxial compression and cyclic loading tests. **b** Typical time history of the loading and strains in lateral strain–controlled uniaxial compression tests. **c** Normalised stress–strain curves of monotonic loading tests. TL tuffeau limestone
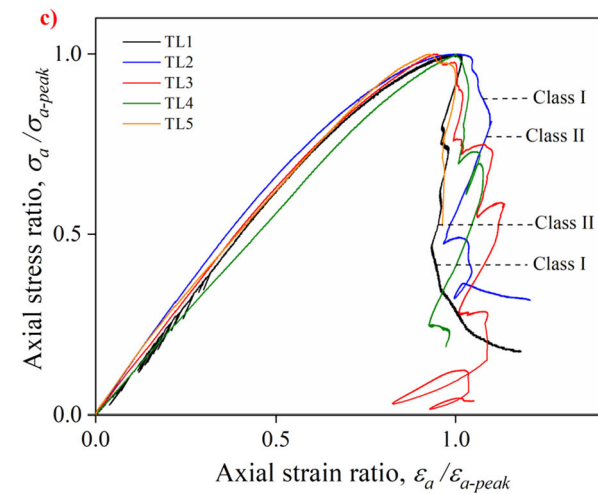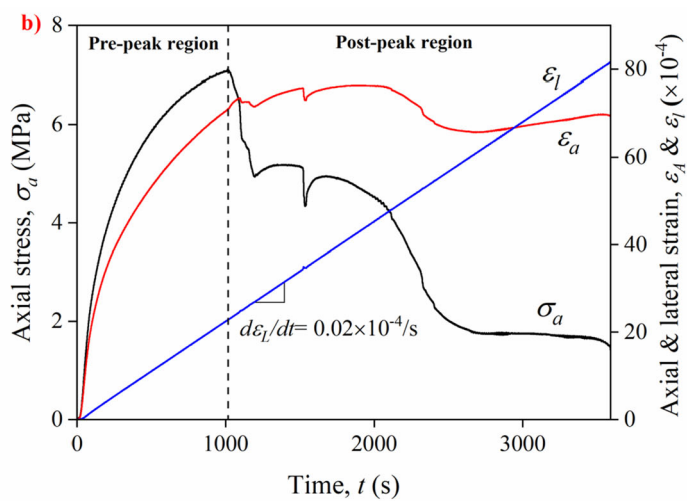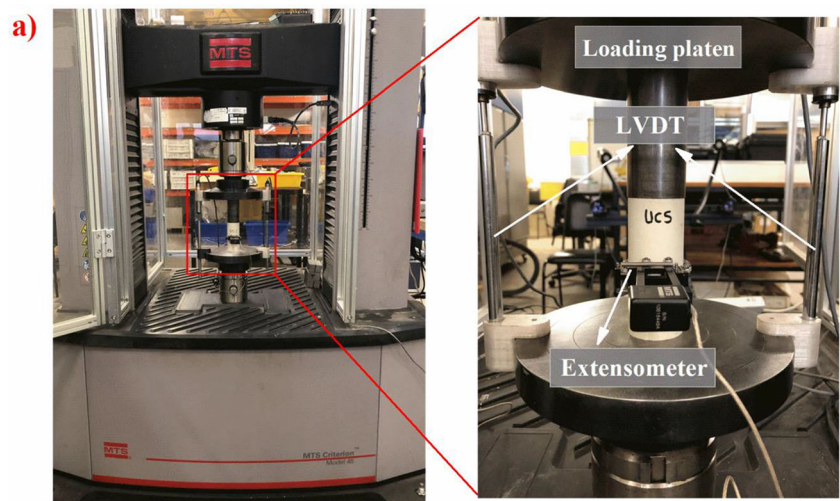
complete post-peak response is obtained in a straightforward manner using the lateral strain–controlled technique. Figure 6 c shows the normalised stress–strain curves obtained from the five uniaxial monotonic tests. The specimens have an average monotonic compressive strength and Young's modulus of 7.39 MPa and 1.67 GPa. As seen from Fig. 6c, in the post-peak region, the axial stress and axial strain fluctuate successively due to the coupled mechanism of strength degradation induced by the coalescence of the macrocracks and strength recovery induced by interlocking the sides of the macrocracks.

However, the total behaviour of all the conducted monotonic tests in the post-peak region is a combination of class I and class II behaviours, which is consistent with the results reported by Munoz et al. (2016a). Additionally, the conducted monotonic tests exhibit similar behaviour both in the pre-peak and the post-peak regions, which shows the low discrepancy among the tested specimens.

Double-criteria damage-controlled cyclic loading test

In this section, an innovative damage-controlled testing method is proposed to capture the post-peak behaviour of tuffeau limestone in a multi-level systematic cyclic loading test. Figure 7 schematically represents the proposed testing methodology during a closed-loop procedure. However, the test procedure can be summarised as follows:

(a)   The specimen is subjected to a monotonic loading under a constant lateral strain rate of 0.02×10^{-4}/s, satisfying quasi-static loading conditions, until a prescribed stress level (here, 6 MPa) is reached. In this stage, the axial stress and lateral strain feedback signals received from the load cell and the chain extensometer, respectively, are continuously compared with the program signals (i.e. the user-defined values) and the errors, if any, are adjusted by the servo controller. By doing so, it is guaranteed that the axial load is always applied under a constant lateral strain rate and that the axial load does not exceed the initial stress level defined for cyclic loading. Thereafter, the specimen is unloaded until the axial stress is equal to 0.07 MPa, ensuring that the specimen is always in complete contact with the loading platens.

(b)   Afterwards, cyclic loading is applied under a constant lateral strain rate for a specific number of cycles (i.e. 400 cycles). Two criteria are adopted to control the failure: a maximum axial stress level that can be achieved and a maximum lateral strain amplitude that a tuffeau limestone specimen is allowed to experience in a cycle during loading, Amp. (ε_l). In this study, the initial maximum stress level (i.e. the first criterion) is adopted to be equal to 6.0 MPa. The optimum values for Amp. (ε_l) and the loading rate ($d\varepsilon_l/dt$) were determined based on a previous study conducted by Munoz and Taheri (2017a) on tuffeau limestone and the results obtained from the trial tests to avoid the sudden failure of a specimen in an uncontrolled manner. Therefore, different loading rates and Amp. (ε_l) values were evaluated by performing four trial cyclic loading tests, and finally, Amp. (ε_l) = 17 × 10^{-4} and $d\varepsilon_l/dt = 2 \times 10^{-4}$/s were obtained by balancing the capability of the methodology in capturing the post-peak behaviour of the rock and completing the test in the shortest possible time. The axial load is reversed when at least one criterion is met. By following the closed-loop

Fig. 7 Flowchart of the double-criteria damage-controlled test method for ▶ the multi-level systematic cyclic loading

procedure shown in Fig. 7, the test is continued until the specimen fails or until 400 cycles are completed.

(c)   If the specimen does not fail after 400 cycles, the specimen is monotonically loaded under a constant lateral strain rate of 0.02×10^{-4}/s until the specimen is under an axial load of 6.5 MPa (i.e. a 0.5 MPa increase in the stress level compared to the previous stress level in this multi-level cycling loading scheme). If the specimen fails during monotonic loading, the complete post-peak behaviour is measured during lateral strain–controlled loading.

(d)   The procedure explained in b and c is repeated until the specimen fails.

Figure 8 shows typical results for a tuffeau limestone specimen. As shown in this figure, after initial monotonic loading under the constant loading rate of 0.02×10^{-4}/s, the prescribed axial stress level (i.e. 6 MPa) is reached. Afterwards, the specimen is unloaded monotonically, and then, cyclic loading is applied under a constant lateral strain rate of 2×10^{-4}/s. At the first step of cyclic loading, the amplitude of lateral strain, Amp. (ε_l), is relatively low (6×10^{-4}/s after 200 cycles), and the first criterion is always met during cyclic loading (i.e. the stress level remaining below 6 MPa). As the specimen does not fail after 400 cycles, the axial load is increased monotonically to the second stress level (i.e. 6.5 MPa), and the cyclic loading procedure is repeated. As shown in Fig. 8, in the second series of cyclic loading at the onset of the failure, the lateral strain amplitude, Amp. (ε_l), is equal to 17×10^{-4}. After this cycle, the second criterion controls the cyclic loading, and the strength degradation during post-peak cyclic loading is observed until complete failure. By doing so, the complete post-peak behaviour of the tuffeau limestone under systematic cyclic loading can be successfully observed.

Experimental results

Complete stress–strain response

In this study, three multi-level systematic cyclic loading tests were conducted using the methodology explained above to evaluate the applicability of the proposed testing method in capturing the failure behaviour of the soft and porous tuffeau limestone. Figure 9 displays the axial stress–strain relations obtained for these tests, in which 6 MPa was defined as the initial stress level, and the specimens were subjected to systematic cyclic loading at different stress levels, taking 0.5 MPa
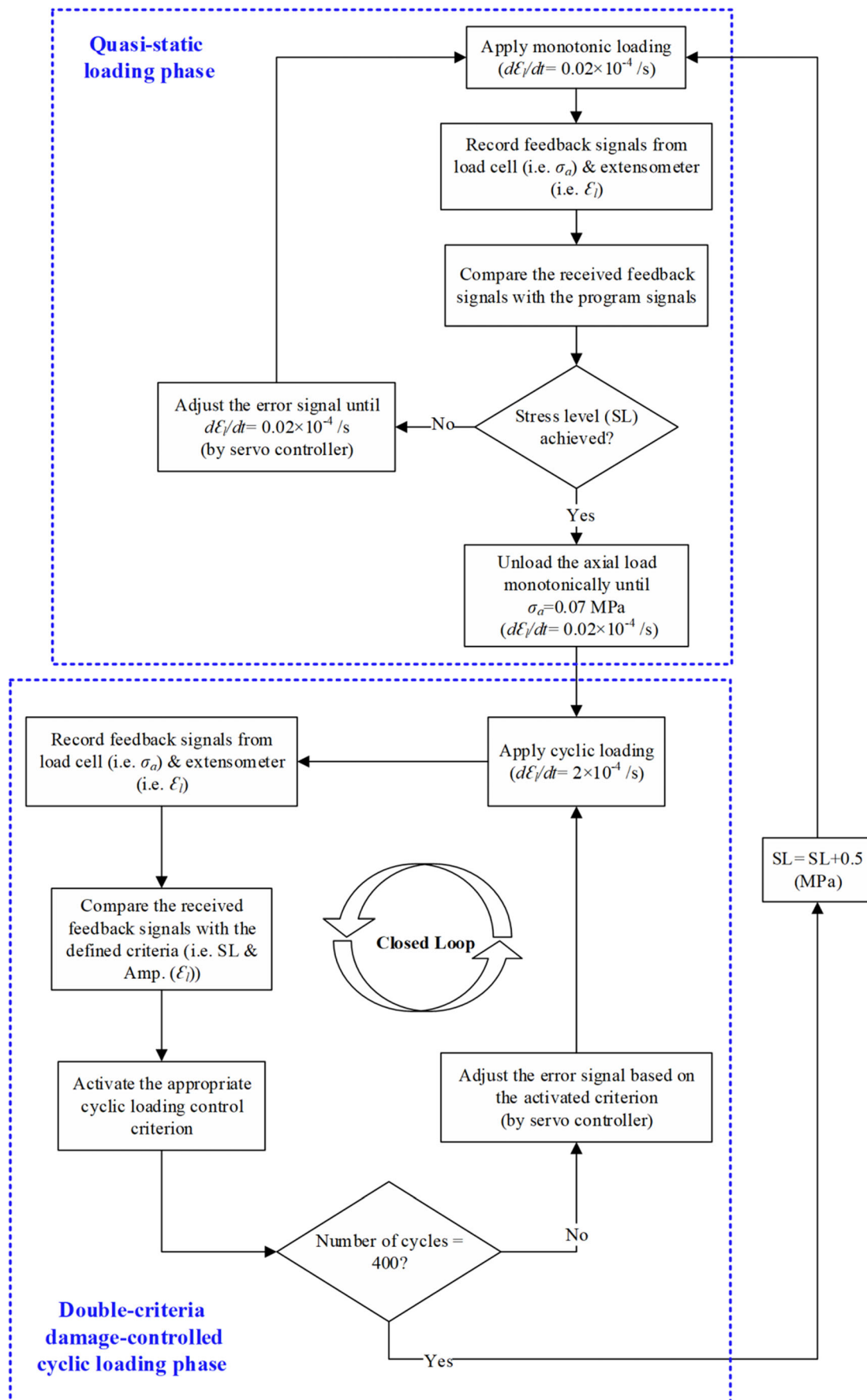
as the stress increment between consecutive cyclic loading steps. The envelope curves showing the overall behaviour of the specimens in the post-peak region were drawn by connecting the loci of the indicator stresses (q_i, the maximum stress of each cycle). As seen from Fig. 9, the overall post-peak behaviour of the specimens is characterised by the combination of class I and class II; however, the class I behaviour is more dominant in specimen TL6 (Fig. 9a) than in specimens TL7 and TL8 (Fig. 9b, c). Table 1 summarises the results of the cyclic loading tests. As listed in Table 1 and shown in Fig. 9, the different cycle numbers and stress levels are recorded for the three specimens before failure; for example, specimen TL8 experienced 2906 cycles before failure, and its failure occurred at a stress level of 9.5 MPa. On the other hand, specimen TL6 exhibited the lowest fatigue strength (i.e. 6.5 MPa) and underwent the fewest number of cycles (i.e. 564) before the failure point. Similar loading conditions were applied to all the specimens, and the results suggest that with the increase in cycle number and thus the loading level before failure, the fatigue strength of the specimens increased and strength hardening occurred. Strength hardening due to cyclic loading has been reported for porous Hawkesbury sandstone (Taheri et al. 2016), hard greywacke sandstone (Singh 1989), Berea sandstone (Burdine 1963) and rock salt (Ma et al. 2013). This phenomenon is discussed in more detail in "Strength hardening behaviour."

Fatigue damage evolution

Damage can be characterised by the process of generation, propagation, and coalescence of mesoscopic defects and voids through solid materials. Damage can be described by the degradation of some material properties, such as stiffness, residual strength, and P wave velocity. Additionally, damage during
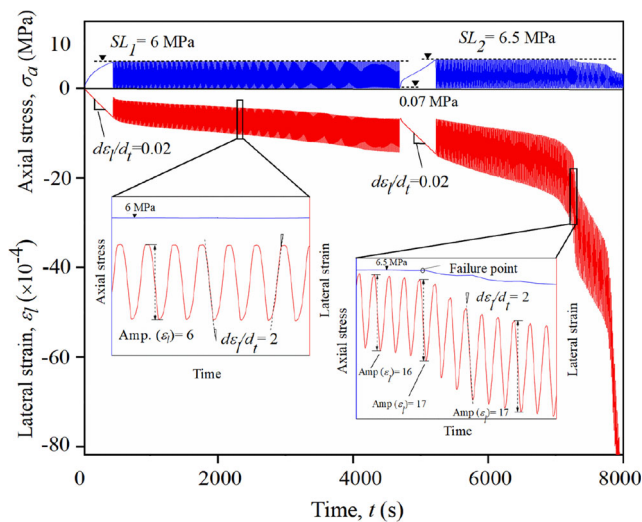

Fig. 8 Typical time history of axial stress and lateral strain during a double-criteria cyclic damage–controlled test

Table 1 Test scheme for the three tuffeau limestone specimens under multi-level systematic cyclic loading

Specimen ID	Stress level	Maximum stress (MPa)	N_{before}	Remark
TL6	1	6	400	Not failed
	2	6.5	164	Failed
TL7	1	6	400	Not failed
	2	6.5	400	Not failed
	3	7	400	Not failed
	4	7.5	115	Failed
TL8	1	6	400	Not failed
	2	6.5	400	Not failed
	3	7	400	Not failed
	4	7.5	400	Not failed
	5	8	400	Not failed
	6	8.5	400	Not failed
	7	9	400	Not failed
	8	9.5	106	Failed

TL tuffeau limestone specimen, N_{before} number of cycles before failure point

cyclic loading can be investigated by the corresponding irreversible strain, dissipative energy, electrical resistance and acoustic emission counts (Xiao et al. 2010; Taheri and Tatsuoka 2012). The incremental accumulation of plastic deformation during cyclic loading contributes to the degradation of the cohesive strength and stiffness of the rocks. Therefore, the irreversible strain can be regarded as a suitable indicator for fatigue damage assessment. Hence, a damage variable (D) was defined based on the accumulation of irreversible axial strain (ε_a^{irr}) (see Fig. 10) after each loading and unloading cycle as follows:

$$D = \frac{\sum_{i=1}^{m} (\varepsilon_a^{irr})_i}{\sum_{i=1}^{n} (\varepsilon_a^{irr})_i} \quad (1)$$

where i is the cycle number, $\sum_{i=1}^{M} (\varepsilon_a^{irr})_i$ is the accumulation of irreversible strain after m cycles, and $\sum_{i=1}^{n} (\varepsilon_a^{irr})_i$ is the total cumulative irreversible strain during the entire multi-level systematic cyclic loading test.

Rock deformability and its failure mechanism are closely related to energy dissipation. Therefore, the energy trends during the rock deformation process can reflect the rock damage mechanism (Zhang et al. 2019b). As shown in Fig. 10, a part of the total work done on the unit volume of a specimen (U_t) by the external force during a loading-unloading cycle is stored in the specimen as elastic energy (U_e); the remaining is released as dissipated energy (U_d) due to plastic deformation
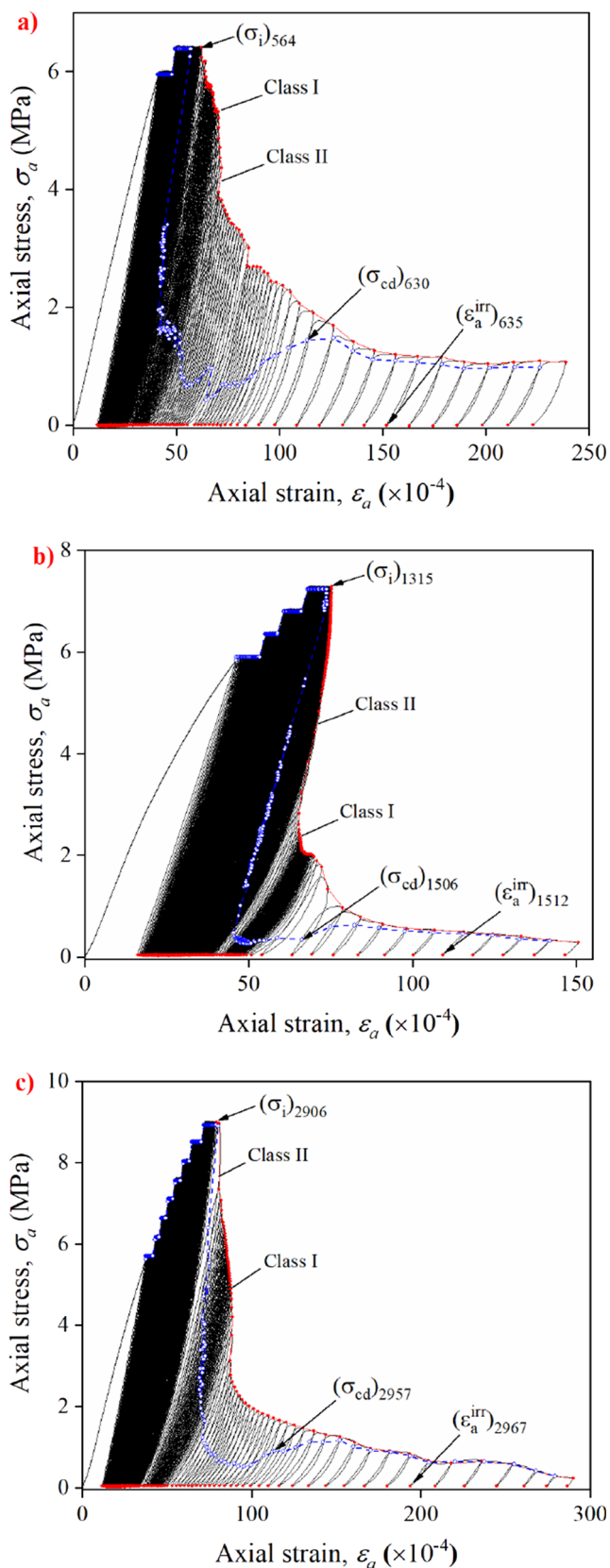
Fig. 9 Complete axial stress–strain relations for tuffeau limestone specimens obtained from cyclic loading tests. **a** TL6. **b** TL7. **d** TL8
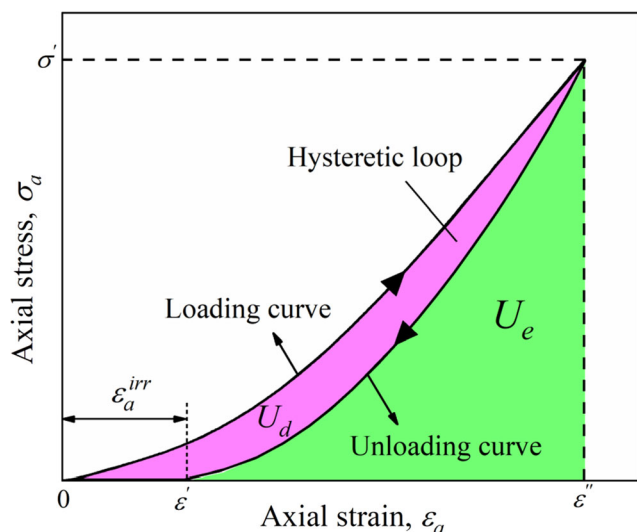

Fig. 10 Distribution of elastic energy (U_e) and dissipated energy (U_d) during a loading-unloading cycle

and rock damage. Because of the complexity in energy conversion during rock deformation and failure, subtle energies (thermal energy, acoustic emission energy, kinetic energy, etc.) are usually ignored to simplify the energy equation as follows (Zhou et al. 2019):

$$U_t = U_e + U_d \tag{2}$$

$$\begin{cases} U_t = \int_0^{\varepsilon_a^{''}} \sigma_a \, d\varepsilon_a \\ U_e = \int_{\varepsilon'}^{\varepsilon_a^{''}} \sigma_a \, d\varepsilon_a \\ U_d = U_t - U_e \end{cases} \tag{3}$$

Figure 11 summarises the evolution of the damage variable (D), elastic modulus (E) and energy dissipation ratio ($K = U_d / U_t$) as damage parameters for specimen TL6. A similar trend was observed for the other tested specimens. As demonstrated in Fig. 11, the total behaviour of damage parameters under
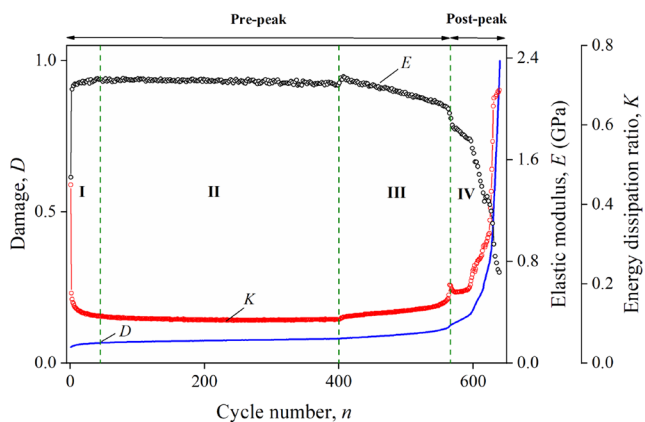

Fig. 11 Typical evolution of damage and stiffness parameters during multi-level systematic cyclic loading of specimen TL6

multi-level systematic cyclic loading conditions can be divided into four stages. In stage I, the damage variable (D) increases slightly and is accompanied by the rapid increase in stiffness (E) from 1.46 to 2.23 GPa, corresponding to the closure of existing defects and expansion of the yield surface (Taheri and Tatsuoka 2015). Furthermore, the energy dissipation ratio (K) decreases suddenly in this stage, which indicates that the elastic energy (U_e) accumulates more rapidly than the dissipated energy (U_d). Stage II, which is the majority of the damage evolution process, shows a nearly unchanging behaviour for all three damage parameters D, E and K. In this stage, although the specimen has experienced 400 cycles, no notable damage is incurred in the specimen. This stage can be interpreted as a balance between the two mechanisms of dilatant microcracking, which reduces the rock stiffness, and grain crushing and pore collapse, which improves the rock stiffness. This balanced state between two competing inelastic procedures results in a quasi-elastic behaviour of the damage parameters in such a way that the deformation seems elastic, and no more energy is dissipated in this stage. In stage III, during the transition to the second stress level via a monotonic loading, the elastic modulus first increases for several cycles. This increase may be related to the change in the strain rate from 2×10^{-4}/s to 0.02×10^{-4}/s for monotonic loading, which allows the existing microcracks and pores to be more compacted and ultimately results in a small stiffening (Peng et al. 2019). Then, the elastic modulus decreases gradually due to the dilatant cracking that degrades the axial stiffness and simultaneously allows more energy to be dissipated (see the trend of K in Fig. 11). In stage IV, the specimen enters the post-peak region due to the coalescence of the microcracks and the generation of macrocracks through the specimen, and the degradation process of the specimen increases dramatically. According to Fig. 11, the energy dissipation ratio (K) and damage variable (D) increase rapidly in this stage, while the stiffness of the specimen decreases until the residual state is reached.

Crack damage threshold stress evolution

The crack damage threshold stress (σ_{cd}), the stress corresponding to the reversal point of volumetric strain at the onset of dilation (Taheri et al. 2020), is an important parameter concerning the unstable damage evolution because it describes the transition of specimen deformation from the compaction-dominated state to the dilatancy-dominated state. As shown in Fig. 9, during cyclic loading at each stress level in the pre-peak stage, σ_{cd} is almost constant and very close to the maximum stress in each cycle. When transitioning to the higher stress levels using a monotonic loading, σ_{cd} increases to reach a stationary state at each stress level. The results presented in Fig. 9 show that by applying 400 cycles at each stress level, the closed microvoids and micropores are not re-

opened during pre-peak cyclic loading until the cyclic loading damages the rock at the last stress level. Thus, when the cyclic loading stress level is not high enough to cause the specimen to fail, the specimen does not switch from a compaction-dominated state to a dilatancy-dominated state but instead acts as an elastic material. According to Fig. 9a, specimen TL6 shows dilatant behaviour in the pre-peak region, in the second cyclic loading stage, by a sudden drop in σ_{cd} due to the re-opening of closed cracks and the generation of new cracks. Degradation of σ_{cd} continues in the post-peak region, followed by strength degradation until the specimen starts to show a residual strength state where σ_{cd} increases to reach a stable condition. For specimens TL7 (Fig. 9b) and TL8 (Fig. 9c), the drop in σ_{cd} occurs very close to and at the failure point, respectively. This, in turn, causes a sudden release of stored elastic strain energy in a self-sustaining manner.

Strength hardening behaviour

As mentioned earlier, in the cyclic loading tests, an increase in the peak strength of specimens TL7 and TL8 was observed with the increase in fatigue life in the pre-peak region. The discrepancy among specimens may partially contribute to this trend in the results. Considering the previous findings (Burdine 1963; Singh 1989; Ma et al. 2013; Taheri et al. 2017) and the results of cyclic loading tests in this study, the authors believe that the increase in the peak strength of specimens TL7 and TL8 is due to not only this discrepancy but also the cyclic loading. This phenomenon should be investigated in future studies by undertaking more specific cyclic loading tests. The hardening behaviour, however, is discussed briefly below.

As discussed in "Fatigue damage evolution" and shown in Fig. 11, during pre-peak systematic cyclic loading, when the stress level is not high enough to cause the specimen to fail due to fatigue, a quasi-elastic behaviour dominates the damage evolution process. In this stage, some mesoscopic elements with lower strength and stiffness may reach their maximum load-bearing capacity, and the weak bonding between the grains breaks, producing fine materials. However, as the stress level is not close to the failure point, due to the slippage and dislocation of the produced fine materials, the existing microfissures and pores are filled during cyclic loading. This may result in more compaction of the specimen and, consequently, strength hardening. This behaviour can also be confirmed by the variation in crack damage threshold stress (σ_{cd}) during cyclic loading (see Fig. 9). As explained in "Crack damage threshold stress evolution," specimen TL8, which experienced more loading and unloading cycles in the pre-peak region than the other specimens did, is mostly in the compaction-dominated stage; dilation occurs at the failure point, followed by the sudden decrease in σ_{cd}. This, in turn,
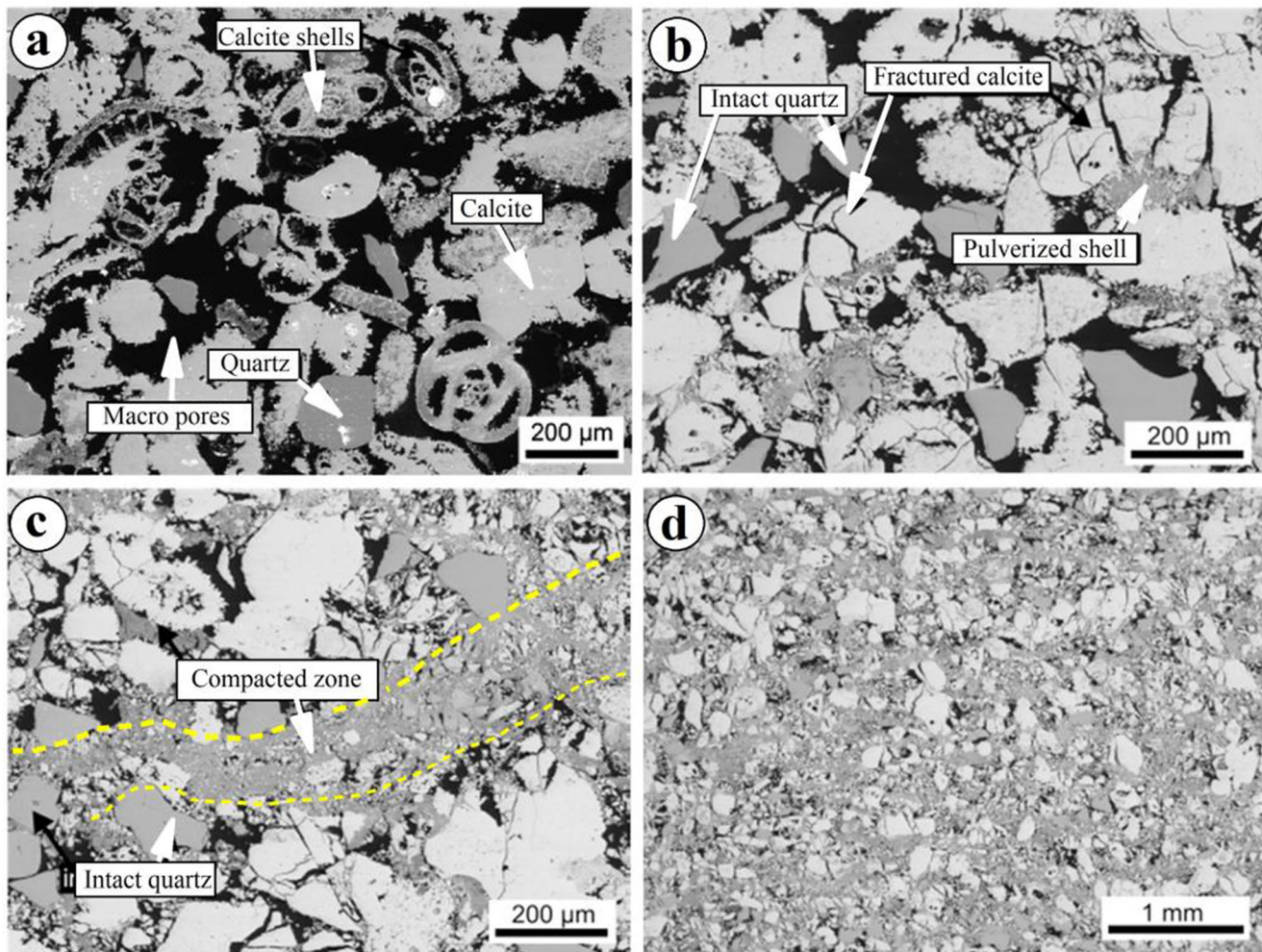
Fig. 12 Backscattered SEM images of a porous limestone in **a** intact and triaxial compression conditions for **b** 14% and **c, d** 27% axial strain (modified from Baud et al. (2017))

resulted in the strength improvement of specimen TL8. However, for specimen TL6 with a shorter fatigue life, dilation occurred earlier in the pre-peak region. The process of rock compaction and porosity reduction in highly porous rock material may be similar to the mechanism explained by Baud et al. (2017). Figure 12 shows the backscattered SEM images of a highly porous limestone in intact and deformed conditions under the same confining pressure of 9 MPa at different axial strain levels. As shown in this figure, when the intact specimen (Fig. 12a) deforms to 14% strain, microcracks are created in the calcite grains, and most of the fossil shells are broken and pulverised, while the quartz grains largely remain intact (Fig. 12b). With the further deformation of the specimen to 27% strain (Fig. 12c), the majority of the calcite grains are broken, and all of the fossil shells are pulverised, resulting in the existing pores being filled and the creation of compacted zones through the specimen. This grain packing is more evident in Fig. 12d, at a larger scale. The stress may concentrate more around the compacted areas, which behave elastically

during loading, and may contribute to the specimens exhibiting more brittle failure.

Conclusions

An innovative testing methodology considering two criteria was proposed in this study to describe the post-peak behaviour of rocks subjected to systematic cyclic loading. Regarding this, the tuffeau limestone was selected to evaluate the capability of the proposed testing method in capturing the full stress–strain response of soft rocks. After obtaining the optimum values for the loading rate ($d\varepsilon_1/dt$) and Amp. (ε_1) during a trial procedure, three main multi-level systematic cyclic loading tests were conducted on tuffeau limestone specimens using the proposed damage-controlled test method. The evolution of different parameters, including the peak strength, damage variable, elastic modulus and crack damage threshold stress, was evaluated comprehensively with the results of the

conducted cyclic loading tests. The following conclusions were drawn from this study:

1. The proposed double-criteria damage-controlled testing method was successful in capturing the class II post-peak behaviour of tuffeau limestone subjected to multi-level systematic cyclic loading. This testing method can provide new insights regarding the damage evolution of rocks in the post-peak region under systematic cyclic loading conditions, which was not previously achievable. The test method was successfully performed on tuffeau limestone, which is a soft rock. The application of the method still needs to be examined on stronger rock types.

2. The whole process of cyclic loading tests conducted in this study can be summarised into several stages: (a) The rock specimen initially stiffens and shows elastic behaviour due to the initial compaction, which is accompanied by the reduction in the energy dissipation; (b) due to a balance between the grain-crushing and pore collapse processes during compaction, a quasi-elastic behaviour dominates the whole test; (c) the stiffness of the specimen decreases gradually due to dilatant microcracking, which dissipates more energy; and (d) with the generation and coalescence of microcracks, the rocks transition from a dilatant state, characterised by the rapid increase in damage and energy dissipation and stiffness reduction.

3. The evolution of the crack damage threshold stress (σ_{cd}) during cyclic loading showed that the specimens do not switch from a compaction-dominated to a dilatancy-dominated state when the cyclic loading stress level is not high enough to cause the specimen to fail. This results in a constant σ_{cd} that is very close to the unloading stress in each cycle.

4. An increase in strength with an increase in fatigue life was observed for the highly porous tuffeau limestone. According to the variation in the damage parameters, stiffness and crack damage threshold stress during the systematic cyclic loading tests, this hardening behaviour can be due to the further compaction of a rock specimen with increasing number of cycles in the pre-peak region. Indeed, the weak bonding between the grains may break down during cycling loading, and the fine materials produced in this process may fill the existing micropores and microfissures, which can result in a porosity reduction and hardening behaviour.

Compliance with ethical standards

Conflict of interest The authors declare that they have no conflict of interest.

References

Akinbinu VA (2016) Class I and class II rocks: implication of self-sustaining fracturing in brittle compression. Geotech Geol Eng 34(3):877–887

Al-Mukhtar M, Beck K (2006) Physical-mechanical characterisation of hydraulic and non-hydraulic lime based mortars for a French porous limestone. arXiv Prepr physics/0609108

Attewell PB, Sandford MR (1974) Intrinsic shear strength of a brittle, anisotropic rock—I: experimental and mechanical interpretation. In: International Journal of Rock Mechanics and Mining Sciences & Geomechanics Abstracts. Elsevier, 11(11):423–430

Bagde MN, Petroš V (2005) Fatigue properties of intact sandstone samples subjected to dynamic uniaxial cyclical loading. Int J Rock Mech Min Sci 42(2):237–250

Baud P, Schubnel A, Heap M, Rolland A (2017) Inelastic compaction in high-porosity limestone monitored using acoustic emissions. J Geophys Res Solid Earth 122:9910–9989

Beck K, Al-Mukhtar M (2014) Cyclic wetting–drying ageing test and patina formation on tuffeau limestone. Environ Earth Sci 71(5): 2361–2372

Burdine NT (1963) Rock failure under dynamic loading conditions. Soc Pet Eng J 3(1):1–8

Cardani G, Meda A (2004) Marble behaviour under monotonic and cyclic loading in tension. Constr Build Mater 18(6):419–424

Cerfontaine B, Collin F (2018) Cyclic and fatigue behaviour of rock materials: review, interpretation and research perspectives. Rock Mech Rock Eng 51(2):391–414

Cho SH, Ogata Y, Kaneko K (2003) Strain-rate dependency of the dynamic tensile strength of rock. Int J Rock Mech Min Sci 40(5):763–777

Eberhardt E, Stead D, Stimpson B (1999) Quantifying progressive pre-peak brittle fracture damage in rock during uniaxial compression. Int J Rock Mech Min Sci 36(3):361–380

Fairhurst CE, Hudson JA (1999) Draft ISRM suggested method for the complete stress-strain curve for intact rock in uniaxial compression. Int J Rock Mech Min Sci 36(3):279–289

Ghamgosar M, Erarslan N (2016) Experimental and numerical studies on development of fracture process zone (FPZ) in rocks under cyclic and static loadings. Rock Mech Rock Eng 49(3):893–908

Guo H, Ji M, Zhang Y, Zhang M (2018) Study of mechanical property of rock under uniaxial cyclic loading and unloading. Adv Civ Eng 2018:1670180

Heap MJ, Faulkner DR, Meredith PG, Vinciguerra S (2010) Elastic moduli evolution and accompanying stress changes with increasing crack damage: implications for stress changes around fault zones and volcanoes during deformation. Geophys J Int 183(1):225–236

Hudson JA, Brown ET, Fairhurst C (1971) Optimising the control of rock failure in servo-controlled laboratory tests. Rock Mech 3(4):217–224

Li T, Pei X, Wang D, Huang R, Tang H (2019) Nonlinear behavior and damage model for fractured rock under cyclic loading based on energy dissipation principle. Eng Fract Mech 206:330–341

Liu J, Xie H, Hou Z, Hou Z, Yang C, Chen L (2014) Damage evolution of rock salt under cyclic loading in unixial tests. Acta Geotech 9(1): 153–160

Ma L, Liu X, Wang M, Xu H, Hua R, Fan P, Jiang S, Wang G, Yi Q (2013) Experimental investigation of the mechanical properties of

rock salt under triaxial cyclic loading. Int J Rock Mech Min Sci 62:34–41

Munoz H, Taheri A (2017a) Local damage and progressive localisation in porous sandstone during cyclic loading. Rock Mech Rock Eng 50(12):3253–3259

Munoz H, Taheri A (2017b) Specimen aspect ratio and progressive field strain development of sandstone under uniaxial compression by three-dimensional digital image correlation. J Rock Mech Geotech Eng 9(4):599–610

Munoz H, Taheri A (2019) Postpeak deformability parameters of localised and nonlocalised damage zones of rocks under cyclic loading. Geotech Test J 42(6):1663–1684

Munoz H, Taheri A, Chanda EK (2016a) Rock drilling performance evaluation by an energy dissipation based rock brittleness index. Rock Mech Rock Eng 49(8):3343–3355

Munoz H, Taheri A, Chanda EK (2016b) Pre-peak and post-peak rock strain characteristics during uniaxial compression by 3D digital image correlation. Rock Mech Rock Eng 49(7):2541–2554

Peng K, Zhou J, Zou Q, Yan F (2019) Deformation characteristics of sandstones during cyclic loading and unloading with varying lower limits of stress under different confining pressures. Int J Fatigue 127:82–100

Singh SK (1989) Fatigue and strain hardening behaviour of graywacke from the flagstaff formation, New South Wales. Eng Geol 26(2):171–179

Taheri A, Tatsuoka F (2012) Stress–strain relations of cement-mixed gravelly soil from multiple-step triaxial compression test results. Soils Found 52(4):748–766

Taheri A, Tatsuoka F (2015) Small- and large-strain behaviour of a cement-treated soil during various loading histories and testing conditions. Acta Geotech 10(1):131–155

Taheri A, Royle A, Yang Z, Zhao Y (2016) Study on variations of peak strength of a sandstone during cyclic loading. Geomech Geophys Geo-Energy Geo-Resources 2(1):1–10

Taheri A, Hamzah N, Dai Q (2017) Degradation and improvement of mechanical properties of rock under triaxial compressive cyclic loading. Japanese Geotech Soc Spec Publ 5:71–78

Taheri A, Zhang Y, Munoz H (2020) Performance of rock crack stress thresholds determination criteria and investigating strength and confining pressure effects. Constr Build Mater 243:118263

Wang S, Xu W, Sun M, Wang W (2019) Experimental investigation of the mechanical properties of fine-grained sandstone in the triaxial cyclic loading test. Environ Earth Sci 78(14):416

Wawersik WR, Fairhurst CH (1970) A study of brittle rock fracture in laboratory compression experiments. In: Int J Rock Mech Min Sci Geomech Abstr . Elsevier, 7(5):561–575

Xiao J-Q, Ding D-X, Xu G, Jiang F-L (2009) Inverted S-shaped model for nonlinear fatigue damage of rock. Int J Rock Mech Min Sci 46(3):643–648

Xiao J-Q, Ding D-X, Jiang F-L, Xu G (2010) Fatigue damage variable and evolution of rock subjected to cyclic loading. Int J Rock Mech Min Sci 47:461–468

Xuefeng X, Linming D, Caiping L, Zhang Y (2010) Frequency spectrum analysis on micro-seismic signal of rock bursts induced by dynamic disturbance. Min Sci Technol 20(5):682–685

Zhang J, Deng H, Taheri A, Ke B, Liu C (2019a) Deterioration and strain energy development of sandstones under quasi-static and dynamic loading after freeze-thaw cycles. Cold Reg Sci Technol 160:252–264

Zhang Y, Zhao T, Taheri A, Tan Y, Fang K (2019b) Damage characteristics of sandstone subjected to pre-peak and post-peak cyclic loading. Acta Geodyn Geromaterialia 16(2):143–151

Zhou HW, Wang ZH, Wang CS, Liu JF (2019) On acoustic emission and post-peak energy evolution in Beishan granite under cyclic loading. Rock Mech Rock Eng 52(1):283–288